Langmuir

Article

pubs.acs.org/Langmuir

Equilibrium Adsorption of Hexahistidine on pH-Responsive Hydrogel Nanofilms

Gabriel S. Longo,[†] Monica Olvera de la Cruz,[‡,§] and Igal Szleifer*[,§,∥,⊥]

[†]Instituto de Investigaciones Fisicoquímicas Teóricas y Aplicadas (INIFTA), CONICET, La Plata, Argentina

[‡]Department of Materials Science and Engineering, [§]Chemistry of Life Processes Institute, [∥]Department of Biomedical Engineering, and [⊥]Department of Chemistry, Northwestern University, Evanston, Illinois 60208, United States

Supporting Information

ABSTRACT: We present a molecular theory to study the adsorption of different species within pH-sensitive hydrogel nanofilms. The theoretical framework allows for a molecular-level description of all the components of the system, and it explicitly accounts for the acid−base equilibrium. We concentrate on the adsorption of hexahistidine, one of the most widely used tags in bio-related systems, particularly in chromatography of proteins. The adsorption of hexahistidine within a grafted polyacid hydrogel film shows a nonmonotonic dependence on the solution pH. Depending on the salt concentration, the density of the polymer network, and the bulk concentration of peptide, substantial adsorption is predicted in the intermediate pH range where both the network and the amino acids are charged. To enhance the electrostatic attractions, the acid−base equilibrium of adsorbed hexahistidine is shifted significantly, increasing the degree of charge of the residues as compared to the bulk solution. Such a shift depends critically on the conditions of the environment at the nanoscale. At the same time, the degree of dissociation of the network becomes that of the isolated acid group in a dilute solution, which means that the network is considerably more charged than when there is no adsorbate molecules. This work provides fundamental information on the physical chemistry behind the adsorption behavior and the response of the hydrogel film. This information can be useful in designing new materials for the purification or separation/immobilization of histidine-tagged proteins.

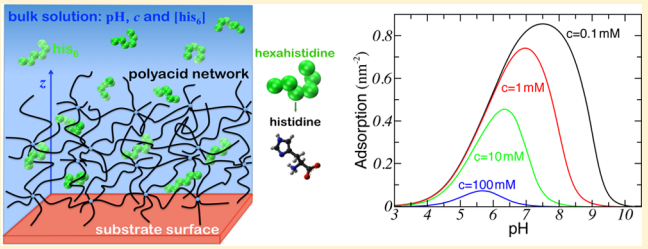

INTRODUCTION

Hydrogels formed by cross-linked pH-sensitive polymer chains display large, reversible volume transitions in response to variations of the acidity of the solution in which they are immersed.[1−3] In addition to the magnitude and reversibility of the externally controlled mechanical response, these materials can be easily designed to be biocompatible, which has made stimuli-responsive hydrogels very attractive for biomaterials research and applications.[4,5] The use of environment-sensitive hydrogels has been investigated for applications in tissue engineering,[6] biosensors,[7−10] and intelligent materials that can mimic biological function.[11] In drug delivery, hydrogels can be used as carriers that encapsulate, within their network, low-molecular-weight antibiotics, DNA and RNA molecules, peptides, proteins, and enzymes.[12−18] For example, the swelling behavior of pH-responsive hydrogels has been investigated for the oral delivery of insulin[19,20] and calcitonin.[21,22]

Protein tags are short peptides attached to proteins for various reasons, which include immobilization and purification from raw biological sources. A histidine oligomer (his-tag) can be incorporated into the primary sequence of recombinant proteins to facilitate their purification from cultures of overexpressing cells using immobilized metal affinity chromatography (IMAC).[23] In this method, introduced by Porath et al.,[24] proteins with the histidine tag reversibly bind to the chromatography matrix that contains chelating ligands. Typically, that matrix is modified with either nitrilotriacetic acid (NTA) or iminodiacetic acid, complexed with metal ions such as cobalt, nickel, copper, or zinc. The most frequently used his-tag in IMAC is that formed by six consecutive histidine residues (his_6). Reversible immobilization of numerous hexahistidine-containing peptides, proteins, and enzymes onto metal-ion-functionalized solid or soft surfaces has been achieved[25−33] as well as the metal-ion-mediated assembly of his_6-tagged proteins onto chitosan fibers.[34] Hydrogels are frequently used as supporting materials for the immobilization of his-tagged proteins.[35,36] For example, the amount of hexahistidine-tagged kinesin bound to the surface of NTA-modified acrylamide hydrogels can be controlled by varying the concentration of the chelating ligand.[35] Supermacroporous poly(acrylamide) cryogels modified with metal affinity matrices have been utilized for the capture and purification of his_6-tagged enzymes using IMAC.[37,38]

The immobilization of biologically relevant macromolecules within the interior of hydrogels presents a number of advantages. The host environment can help enzymes retain

Received: October 12, 2014
Revised: November 29, 2014
Published: December 1, 2014

their activity, stabilizing them against thermally induced denaturation and aggregation, as well as promote refolding of acid-denatured proteins.[39,40] Therefore, hydrogels are excellent candidates for the development of new materials that can serve as the biocompatible matrix for the chromatography of biomolecules. Immobilization and purification of his_6-tagged proteins and enzymes within nickel functionalized poly(2-acetamidoacrylic acid) hydrogels have been demonstrated.[41−43] Poly(ethylene glycol) hydrogels, whose polymer network has been modified with ligands for metal affinity, have been used for the controlled binding and release of hexahistidine-tagged proteins.[44,45] Moreover, using the high affinity between histidine residues and a metal-ion complex, his-tagged rhamnosidase was immobilized within calcium alginate hydrogel beads.[46]

As stated in the previous paragraph, pH-sensitive hydrogels have been recently applied to design full three-dimensional environments suitable for the manipulation of proteins.[41−43,46] Although the physical properties of these materials can be externally tuned by simply changing the composition of the solvent, this responsive behavior has not been exploited in the separation/immobilization of proteins. The long-term motivation for this work is to investigate the possibility of using the solution to enhance or control the adsorption of biomolecules into pH-responsive hydrogels. Thus, we begin by studying the adsorption of different molecules within a surface-grafted polyacid hydrogel film using a theory that allows for a molecular-level description of all the components of the system. In addition, the approach explicitly accounts for the elasticity of the polymer network, the electrostatic and van der Waals interactions, solvent confinement effects, and the chemical free energy that accounts for the acid−base equilibrium of all the titratable components of the system, including those of the network. We delineate some general aspects of the adsorption of molecules within the pH-sensitive film but concentrate our attention on the adsorption of hexahistidine and other his-tags. The theory also describes charge regulation by histidine residues due to the local variations of the environment.

In most experimental works, the specific binding interaction between histidine residues and metal ions is used for the immobilization of the his_6-tagged proteins. In the present work, we investigate the behavior when the adsorption is due to electrostatic attractions between ionized network units and charged histidine residues. Our hypothesis is that the pH sensitivity of the hydrogel can be useful to drive his-tagged proteins to the immobilization matrix thorough controlling the environment. Moreover, the physics and chemistry in the absence of the metal ions are critical in determining the state and amount of his-tag that will be found inside the gel. Therefore, the proper understanding of the adsorption of his-tag driven by electrostatic attractions is of primary importance for the design of applications and for the comprehension of the interplay between adsorption and binding. As we will show, the behavior of the system in the absence of the metal ions is complex, requiring its fundamental understanding before addressing the competition between acid−base equilibrium and ligand−receptor binding.

In a salt solution without adsorbate, the polyacid hydrogel swells as the pH of the medium is raised because the polymeric structure becomes increasingly charged. Swelling occurs to lengthen the distance between confined network charges and reduce the intranetwork electrostatic repulsions. To reduce those repulsions more, the degree of charge of the network is significantly smaller than that expected from ideal solution considerations.[47,48] Depending on the salt concentration, the hydrogel can be weakly charged for pH values well above the intrinsic pK_a of the acidic units of the network (e.g., acrylic acid with pK_a around 5). At the same time, from analogous solution considerations, histidine residues (with basic intrinsic pK_a around 6) are expected to be uncharged in the range of pH where the network is significantly charged. Therefore, it is not clear *a priori* that network−histidine electrostatic attractions can result in significant amounts of adsorption. In the current study, we show that the adsorption shifts the acid−base equilibrium of histidine residues dramatically, as compared to the ideal solution, so that the amino acids remain charged even at high pH. Moreover, the acidic network groups are charged at much lower pH values than in the absence of the peptide. Both phenomena produce and at the same time are also the consequence of considerable amounts of adsorption at a wide range of pH.

RESULTS

In this work, we present theoretical predictions for the adsorption of different molecular species within a pH-responsive hydrogel nanofilm. We use a theory that combines the explicit description of charge regulation with the incorporation of specific molecular details of the polymer network and solution species. The state of charge of the ionizable groups of the network and that of the adsorbate units are locally determined by the interplay between all of the free energy contributions that include the chemical free energy (acid−base equilibrium of the different titratable units), the configurational degrees of freedom of the network, the entropy loss of solvent and ion confinement, and the van der Waals, steric, and electrostatic interactions. The basic idea of this theoretical approach is to write the free energy of the system in terms of the probability of each of the possible spatial conformations of the polymer network and include all the relevant repulsive and attractive interactions together with the different chemical states of the ionizable species. The optimization of the free energy provides the probability of each of the conformers, the state of protonation for each acidic/basic group of the network and adsorbate molecule, and the electrostatic and other interaction potentials. Thus, the theory does not assume the thermodynamic state of either the hydrogel film (network degree of charge, thickness, amount of molecules adsorbed) or the adsorbate species (configuration, local concentration and state of charge). The properties of the system and its components result from the minimal free energy for each set of experimentally controllable variables, namely, the pH, salt concentration, c, and the bulk concentration of the adsorbate, $[a]$. A detailed presentation of the theory and the optimization procedure are presented in the Methods section and more completely in the Supporting Information.

The molecular model used to describe the system is illustrated in Figure 1. The network is composed of cross-linked monodisperse polyacid chains interconnected at six-coordinated nodal monomers (cross-links). Each chain in the network has 25 monomers (excluding the cross-links). Most of the polymer chains connect two cross-links, except topmost chains that have their solution-side ends free and some chains that have one of their ends grafted to fixed positions on the planar surface. Grafting points are arranged in a square lattice with area density σ. The logarithmic acidity constant of a

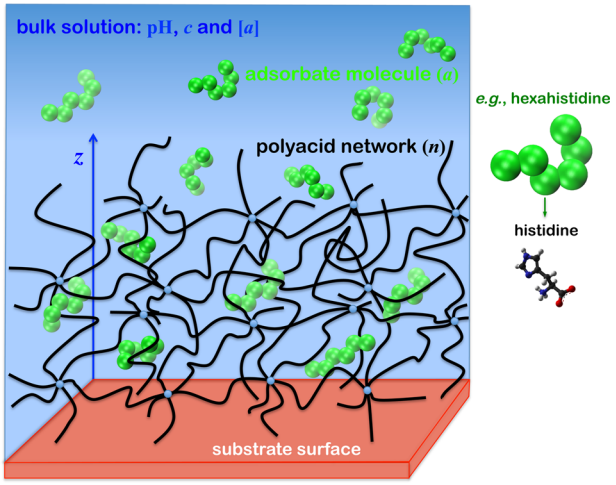

Figure 1. Schematic representation of the system of interest. The picture illustrates a surface-grafted polymer network that can adsorb hexahistidine (or other solute molecules) from a solution with controlled pH, salt concentration, c, and adsorbate concentration, $[a]$. The pH-responsive network is composed of cross-linked polymer chains, each having 25 acidic segments with acidity constant given by $pK_n = 5$. All units of the network are spherical and have the same diameter (segment length), $l_n = 0.5$ nm, and molecular volume, $\nu_n = (\pi/6)l_n^3 = 0.0655$ nm^3. Each histidine residue is represented by a single bead centered at the position of the C_α with a basic acidity constant given by $pK_a = 6$. The bond length of each bead is taken as $l_a = 0.5$ nm, which gives the effective distance between neighboring centers of two unified groups, and its molecular volume is $\nu_a = 0.15$ nm^3.

titratable group of the network is taken as $pK_n = 5$ to model a carboxylic acid such as acrylic acid.[49] Thus, the adsorbent material can represent a poly(acrylic acid) hydrogel nanofilm that is chemically grafted to a solid surface. The molecular model of the polymer network is more extensively described in the Supporting Information as well as in our previous work.[48] The different molecular conformations of the polymer network that serve as input of our theoretical approach are obtained using molecular dynamics simulations. We concentrate in the adsorption of oligomers of histidine (his_n). Each residue of the his_n is represented by a single bead centered at the position of the C_α with a basic $pK_a = 6$.[49] The different conformations of these oligomers are also an input of the molecular theory. These conformations are obtained using a rotational isomeric state model in which each bond can assume one of three possible isoenergetic configurations.[50] Within this model, we generate (and include in the calculations) all the possible conformations of each of the histidine oligomers considered.

We begin presenting results by describing the adsorption of different molecular species inside the hydrogel nanofilm. To this end, it is convenient to define the adsorption

$$\Gamma = \int_0^\infty dz(\langle\rho_a(z)\rangle - \rho_a) \quad (1)$$

which gives the excess amount of adsorbed molecules per unit area. In this definition, ρ_a is the bulk number density of adsorbate, and $\langle\rho_a(z)\rangle$ gives the local number density at a distance z from the surface (both inside and outside the film), such that $\lim_{z\to\infty}\langle\rho_a(z)\rangle = \rho_a$. The angle brackets in the local density represent a position-dependent ensemble average over the adsorbate conformations. The adsorption quantifies not only the excess amount of molecules partitioned in the interior of the network but also considers contributions from the interfacial network-solvent region. Figure 2A shows the dependence of the adsorption on the pH for several spherical nanoparticles with different permanent charge. These results are included to serve as a reference when discussing the adsorption of histidine and oligomers of such amino acid. We find that the adsorption of these spherical molecules depends on the pH due to the different charge states of the hydrogel network. The adsorption of positively charged species grows as the pH increases. The more positive charge the adsorbate nanoparticle carries, the more it adsorbs into the hydrogel at sufficiently high pH. Negatively charged molecules are excluded from the film as the pH increases. This depletion ($\Gamma < 0$) is more significant as the absolute value of the negative charge in the particle increases. No adsorption ($\Gamma \approx 0$) is predicted when the species is electroneutral. Therefore, the Γ profiles of Figure 2A for permanently charged particles clearly show that the driving force for the adsorption (depletion) are the network−adsorbate electrostatic attractions (repulsions).

Panel A of Figure 2 also shows the adsorption of aspartic acid ($pK_a = 3.7$) and histidine ($pK_a = 6$). The adsorption of aspartic

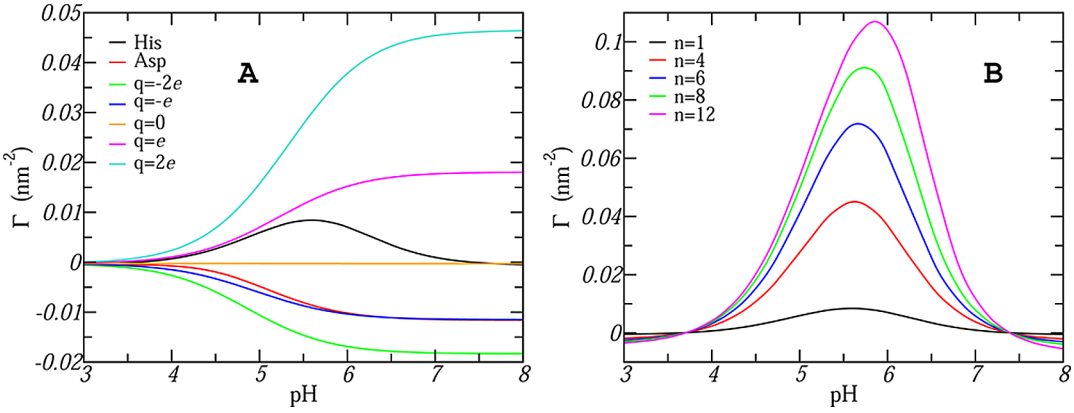

Figure 2. Adsorption, Γ, as a function of the solution pH, for various adsorbate species, which include (A) different nanoparticles with permanent charge q, aspartic acid, and histidine, as well as (B) several n-mers of oligohistidine. Aspartic acid is modeled as having the same diameter as a histidine molecule, $l_a = 0.5$ nm, volume $\nu_a = 0.12$ nm^3, and $pK_a = 3.7$. The permanently charged molecules are spherical particles with a diameter equal to that of a histidine residue to allow for direct comparison, and volume $\nu_a = \pi(l_a^3/6)$. In all cases, the bulk concentration of the adsorbate molecule is 1 mM, the salt concentration is $c = 100$ mM, and the network grafting density is $\sigma = 0.012$ nm^{-2}.

dx.doi.org/10.1021/la5040382 | Langmuir 2014, 30, 15335−15344

acid is not qualitatively different from that of a molecule with a permanent negative charge. This is because the pK_a of the acidic groups of the network and that of the adsorbate molecules are relatively close to each other. Then, at the same conditions that the polymer network can repel like-charged species, aspartic acid is significantly negatively charged and therefore repelled from the nanofilm. The adsorption of a monomer of histidine inside the polyacid film presents a nonmonotonic dependence on the solution pH. At low pH, the network is only weakly ionized, which results in no driving force for the adsorption. At high pH, histidine residues are uncharged, resulting again in negligible adsorption. At intermediate values of pH, however, both the network and the amino acids are significantly charged, leading to an adsorption that displays a maximum at a pH in between the pK_a of the two titratable species. The same qualitative behavior is observed for different histidine oligomers as can be observed in Figure 2B, although the magnitude of the adsorption depends critically on the degree of oligomerization. At both extremes of the pH axis, the electrostatic attractions between the peptide and the network are not sufficient to drive the adsorption because either the network (at low pH) or the adsorbate (at high pH) is weakly charged. In these regions, no adsorption or even depletion is predicted, depending on the size of the peptide. The longer the peptide, the stronger the steric repulsions inside the hydrogel and the more depletion of adsorbates from the network at low or high pH.

We now concentrate our attention on the adsorption of hexahistidine. The reason is twofold. First, his_6 is the most frequently used protein tag for the immobilization and purification of recombinant proteins. Second, the adsorption behavior is qualitatively similar for all the *n*-mers considered in Figure 2B. Figure 3 presents Γ vs pH curves for different

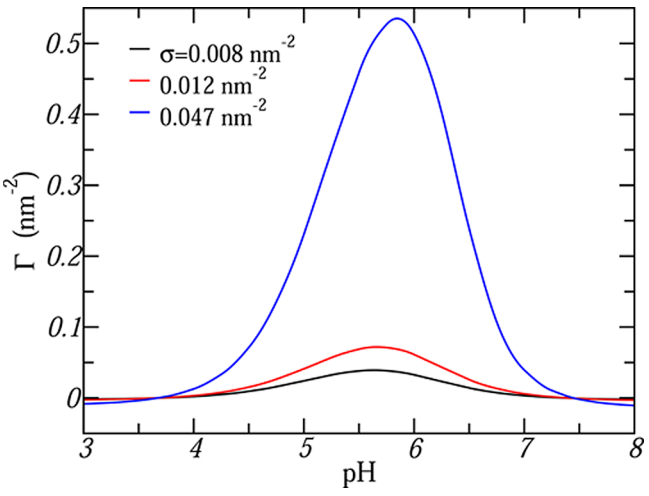

Figure 3. Adsorption of his_6 as a function of the pH for different grafting densities of the polymer network, σ. The bulk concentration of the peptide is [his_6] = 1 mM, and the salt concentration is *c* = 100 mM.

grafting densities of the hydrogel network. The Γ−pH profiles are qualitatively similar for all the different grafting densities, although the quantitative adsorption depends critically on σ. A larger grafting density implies more density of polymer within the film and more electric charge on the network (per unit area) to drive the adsorption of the hexamer. Then, at intermediate pH, the adsorption is significantly enhanced by increasing the grafting density.

Next, we investigate the influence of the bulk concentration of his_6 on the absorption behavior. Adsorption (Γ−pH) profiles at different bulk concentrations are shown in Figure 4A, and adsorption isotherms are presented in panel B of the figure. At low (pH $\lesssim$ 4) or high pH (pH $\gtrsim$7.5), either negligible adsorption or depletion is predicted in the range of concentrations studied, as can be observed in both panels of Figure 4. Under such conditions, adding [his_6] to the solution reduces the adsorption monotonically. This behavior is because Γ is an excess quantity measured relative to the increasing bulk concentration of hexahistidine, and there are no network−histidine electrostatic attractions to drive the adsorption. Histidine is positively charged at low pH, but the network is only weakly charged under this condition. On the contrary, at high pH the polymer matrix is negatively charged but histidine is weakly charged. In the range of pH values where significant adsorption is observed (i.e., when the polymer network is negatively ionized and the adsorbate positively charged), the isotherms shown in Figure 4B display a nonmonotonic behavior. When [his_6] is raised in the bath solution, Γ increases until reaching a maximum at a given concentration in between 0.01 and 0.1 M depending on the pH. Increasing concentration of his_6 further results in less adsorption. This maximum occurs roughly when the charge of the network is completely balanced by that of adsorbed hexahistidine. At higher his_6 concentrations, the network loses the ability to adsorb his_6 through electrostatic attractions. On the contrary, adsorbed hexahistidine residues drive the incorporation of significant amounts of salt anions to neutralize the total charge of the film (see Supporting Information).

The Γ−pH profiles presented in Figure 4A are asymmetric with substantially more depletion of hexahistidine at high than at low pH. This behavior can be more clearly observed for [his_6] = 10 mM (blue curve in Figure 4A), but it is a general feature of these profiles. Such result is interesting since the film is swollen at high pH (see Figure 6), having more available volume in the interior of network to adsorb peptide. However, because the network is strongly charged under this condition, the more favorable situation is for the hydrogel film to use the extra volume to adsorb ionic species that can screen the intranetwork electrostatic repulsions. This adsorption of ions results in the expulsion of the mostly uncharged hexahistidine molecules.

We analyze next the adsorption of his_6 inside the hydrogel film and study the charging behavior of both components (i.e., the polymer network and the adsorbate species) as well as the ability of the structure to swell in the presence of hexahistidine. We begin by describing the ionization of the polymer matrix. The average degree of dissociation of network units can be calculated using

$$\langle f_{gel} \rangle = \frac{\int_0^\infty dz\, f_n(z)\langle \rho_n(z)\rangle}{\int_0^\infty dz\, \langle \rho_n(z)\rangle} \qquad (2)$$

where $\langle \rho_n(z)\rangle$ is the ensemble average of the local density of network segments and $f_n(z)$ is the local degree of charge. Figure 5 shows the average degree of dissociation of the network as a function of the solution pH and salt concentration for two different situations, depending on whether the solution contains hexahistidine (A) or not (B). The dashed lines in the

dx.doi.org/10.1021/la5040382 | *Langmuir* 2014, 30, 15335−15344

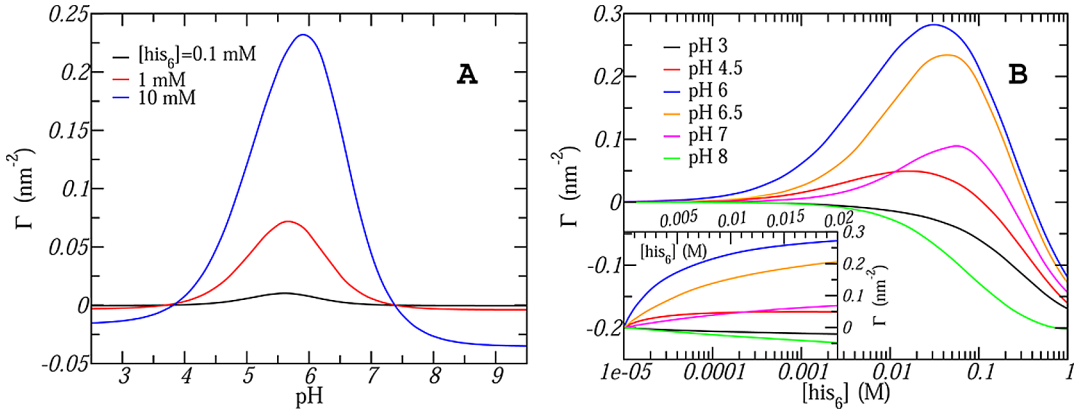

Figure 4. (A) Adsorption vs pH for different bulk concentrations of hexahistidine, [his$_6$]. (B) Adsorption isotherms, Γ, as a function of [his$_6$], for several values of the solution pH. A zoom-in of the isotherms for low bulk concentrations is shown in the bottom-left inset. In both panels, σ = 0.012 nm^{-2} and c = 100 mM.

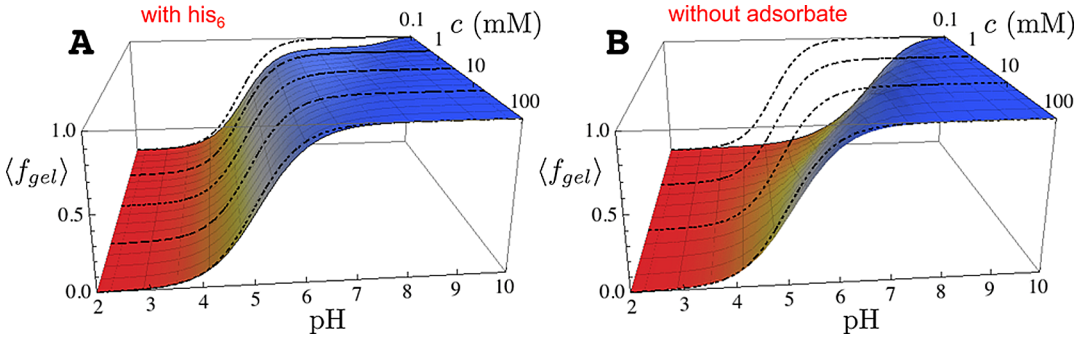

Figure 5. Average degree of dissociation of the network as a function of the solution pH and salt concentration, for a bath solution containing 1 mM of his$_6$ (A) and for a solution that contains no hexahistidine (B). The polymer network is the same in both situations, with a grafting density of σ = 0.012 nm^{-2}.

graphs correspond to the ideal solution titration of acid groups, i.e.

$$f_n^b = \frac{1}{1 + 10^{pK_n - pH}} \quad (3)$$

with pK_n = 5.

The chemical free energy of the network describes the free energy contribution of the acid−base equilibrium of titratable units of the gel. A necessary condition to minimize such contribution to the free energy is that $\langle f_{gel}\rangle = f_n^b$. When the bath solution contains no adsorbate molecules, however, $\langle f_{gel}\rangle$ is significantly lower than f_n^b in a wide range of conditions, but most notably at low c, as can be observed in Figure 5B. This deviation implies that the chemical free energy of the network is far from optimal. The reason for this behavior is that a lower degree of charge on the network reduces the energetic cost due to the electrostatic repulsions arising mostly from counterion confinement. The behavior of this hydrogel, particularly its swelling state, is mainly determined by the competition between the intranetwork electrostatic repulsions and the chemical free energy. When the pH of the solution is raised, the acid−base equilibrium drives the increase of the network degree of charge. In response, the hydrogel swells to lengthen the effective distance between charged network segments and reduce the strength of the electrostatic repulsions.

The competition between the aforementioned physicochemical interactions is modulated by the concentration of monovalent salt. In addition to swelling, the hydrogel can adsorb salt ions, which screen the electrostatic repulsions between charged network units, thus shortening the effective range of those interactions. However, the adsorption of salt ions plays an additional and opposing role. A larger screening of the electrostatic repulsions allows for more dissociation in the network in order to reduce the chemical free energy further, since $\langle f_{gel}\rangle$ is lower than f_n^b.

One of the consequences of this dual role played by salt ions is that the hydrogel film displays a nonmonotonic swelling behavior when the bath solution does not contain hexahistidine. In such situation, there is a range of solution compositions where the film deswells as the bath pH increases[48] (see Figure 6). On the contrary, if the bath solution does contain hexahistidine, $\langle f_{gel}\rangle \approx f_n^b$ under most external conditions (except for a small but appreciable deviation at very low c) as can be seen in Figure 5A. The minimum of the chemical free energy of the network requires $\langle f_{gel}\rangle \approx f_n^b$, as previously mentioned. Then, the results presented in Figure 5A suggest that the contribution to the free energy from the acid−base equilibrium of titratable network units is nearly ideal.

Next we consider how this nearly ideal charging behavior of the network, due to the presence of hexahistidine, modifies the pH-triggered swelling of the film. Some of the polymer chains of the gel are chemically grafted to the supporting surface. Therefore, the film can only swell in the direction perpendicular to the plane of the surface. The only relevant dimension of the film is its thickness, which is defined as twice the first moment of the density distribution of polymer:

dx.doi.org/10.1021/la5040382 | Langmuir 2014, 30, 15335−15344

$$h_{gel} = \frac{\int_0^\infty dz\ (2z)\langle \rho_n(z)\rangle}{\int_0^\infty dz\ \langle \rho_n(z)\rangle} \quad (4)$$

When the gel is in contact with a salt solution, the thickness of the film is a nonmonotonic function of the pH, except at high c, as can be observed in Figure 6 (dotted-line curves). As already discussed, this behavior results from the two opposing roles that the adsorption of salt ions plays in modulating the competition between the acid−base equilibrium of titratable units of the network and the electrostatic repulsions between its charged segments.[48] When the conditions are such that there is no competition between these free energy contributions, the thickness of the film is a monotonic function of the pH. In the case of the solution containing hexahistidine, the degree of dissociation of the polymer gel is almost ideal (see Figure 5A). Since the chemical free energy of the network is near its minimum value, there is no competition with other interactions. As a result, the thickness of the film is mostly a nondecreasing function of the solution pH, as observed in Figure 6 (solid-line curves), although a small region of deswelling is observed with increasing pH.

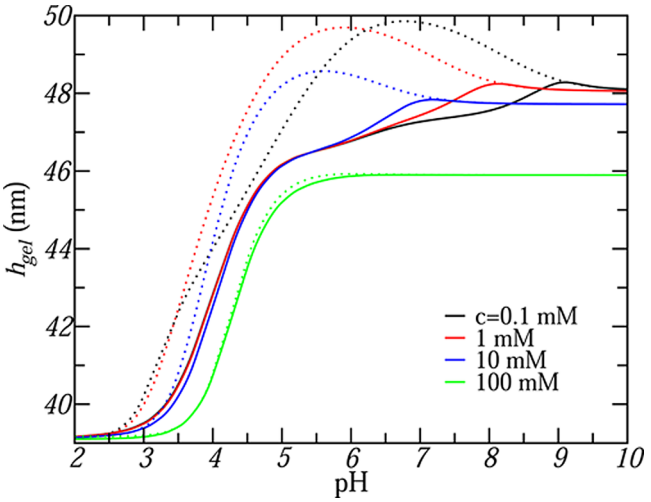

Figure 6. Nanofilm thickness as a function of the pH for solutions containing 1 mM of his_6 and different salt concentrations (solid-line curves). The network grafting density is 0.012 nm^{-2}. The thickness of the film at identical conditions when the bath solution contains no adsorbate species is represented using dotted lines.

Let us now investigate the influence of the solution salt concentration on the adsorption of hexahistidine. Figure 7A presents Γ−pH profiles for different salt concentrations, which display several interesting features. First, his_6 adsorption significantly diminishes as c increases due to the more intense screening by salt ions of the electrostatic attractions between network and histidine units, which is the main driving force for the adsorption. The second intriguing observation is that the range of pH where significant adsorption is predicted grows with decreasing c. This result can be rationalized by looking at Figure 7B, which depicts the average degree of association (charge) of histidine units that are adsorbed inside the film, defined as

$$\langle f_{his}\rangle = \frac{1}{h_{gel}}\int_0^{h_{gel}} dz\, f_{his}(z) \quad (5)$$

where $f_{his}(z)$ is the local degree of charge of histidine units at a distance z from the supporting surface. In addition, Figure 7B shows the degree of charge of the species in the bulk solution, given by

$$f_{his}^b = \frac{1}{1 + 10^{pH - pK_{his}}} \quad (6)$$

with $pK_{his} = 6$. Similarly to the bulk solution behavior, adsorbed histidine residues are strongly charged ($\langle f_{his}\rangle \approx 1$) at low pH and weakly charged at high pH ($\langle f_{his}\rangle \approx 0$). However, the degree of charge of histidine is larger inside the film than in the bulk solution, independently of the pH. As c decreases, more units of the adsorbed hexahistidine molecules are charged, which implies that $\langle f_{his}\rangle$ deviates further from f_{his}^b, especially at high pH. Lowering the salt concentration broadens the pH-dependent discharging transition of adsorbed hexahistidine because the condition of uncharged residues is obtained at higher pH values. Such response of hexahistidine with decreasing c results in more adsorption (Figure 7A) due to the stronger electrostatic attractions with the oppositely charged network units. Not only more residues are charged with a lower c but also the electrostatic attractions are longer

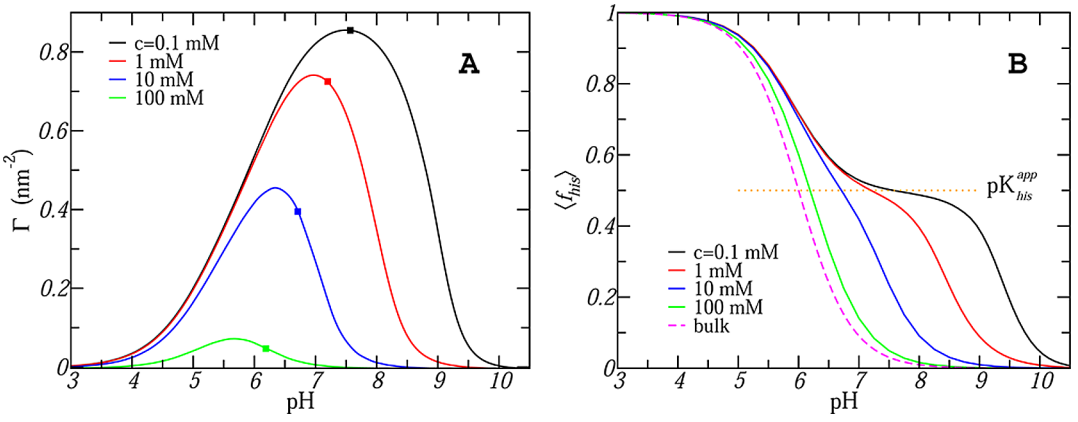

Figure 7. (A) Adsorption as a function of the pH for bath solutions having different salt concentrations and $[his_6]$ = 1 mM. The squares along the curves give the adsorption value when pH = pK_{his}^{app}, the apparent pK_a of adsorbed histidine residues. At this value of pH, exactly half of the adsorbed histidine units are protonated (charged). (B) Average degree of charge of adsorbed his_6 as a function of the solution pH for various c as well as the degree of charge of a histidine residue in the bulk solution (dashed magenta curve). The grafting density of the network is σ = 0.012 nm^{-2}.

dx.doi.org/10.1021/la5040382 | Langmuir 2014, 30, 15335−15344

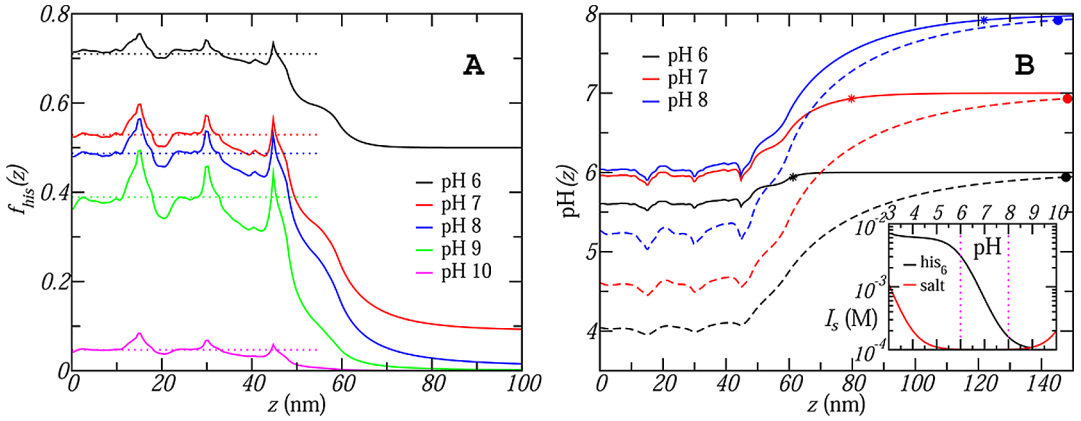

Figure 8. (A) Local degree of charge of histidine residues, $f_{his}(z)$, as a function of the distance from the supporting surface, z, for several pH values. Dotted lines give the average degree of charge inside the film, $\langle f_{his}\rangle$. The bulk solution contains [his$_6$] = 1 mM and c = 1 mM, and the network grafting density is σ = 0.012 nm^{-2}. (B) Local pH, pH(z), as a function of z for different values of the solution pH, at the same conditions of panel A (solid-line curves). Panel B also shows pH(z) for a system at otherwise identical conditions but whose bath solution contains no adsorbate molecules (dashed-line curves). Either a star or a circle along the curve, depending on whether the solution contains or not his$_6$ respectively, marks the distance from the surface at which the local and bulk pH differ from each other by less than 1%. The bottom-right inset shows the bulk ionic strength, I_s, as a function of the pH for both salt and hexahistidine solutions, at the same c as the main plot.

ranged. Then, this broadening of the deprotonation transition of adsorbed his$_6$ units as a function of pH explains why the Γ profiles widens as the salt concentration decreases.

The pH-dependent discharging of adsorbed histidine residues can be further characterized using the apparent pK_a, pK_{his}^{app}, which gives the midpoint of the transition. When pH = pK_{his}^{app}, exactly half of the adsorbed histidine units are protonated (charged). In Figure 7B, the apparent pK_a is marked by the intersection between the corresponding $\langle f_{his}\rangle$−pH curve for a given c and a horizontal line at $\langle f_{his}\rangle$ = 0.5 (orange dotted line). In Figure 7A, pK_{his}^{app} is represented by a square along the Γ profile. At low pH, $\langle f_{his}\rangle$ is relatively close to f_{his}^{b} for all salt concentrations. As the pH approaches pK_{his}^{app}, the degree of charge begins to deviate from its bulk value, an effect that is more noticeable as c decreases. Under such conditions (pH ∼ pK_{his}^{app}), both the network and the adsorbate molecules are significantly charged. The electrostatic energy is reduced by increasing the number of network−histidine attractions. Thus, the equilibrium conditions are shifted to a higher degree of charge in the hexamer as compared to the bulk value. At low salt concentration, the electrostatic interactions are long-ranged, which makes the shift more pronounced. In particular, at the lowest c shown in Figure 7B, this effect occurs to such an extent that $\langle f_{his}\rangle$ nearly plateaus for more than 1 unit of pH around its apparent pK_a. This asymmetry of the different $\langle f_{his}\rangle$−pH profiles is also present in the Γ profiles of panel A, which are wider as c decreases. As a consequence, the pH of maximal adsorption, which occurs near pK_{his}^{app} (see squares in Figure 6), shifts to higher values as c decreases.

Additional information on the charging behavior of his$_6$ is presented in Figure 8A, which shows the local degree of charge of peptide units as a function of the distance from the surface. Three regions can be clearly defined in the graph. Inside the film ($0 < z \leq h_{gel} \sim 50$ nm), the local degree of charge takes values that average to $\langle f_{his}\rangle$ (represented by dotted lines in the figure). The spikes observed in this region, which occur regularly spaced, correspond to the position of the network cross-links which have, consequently, the highest density of polymer. Around these positions, histidine residues are slightly more charged due to the higher density of localized negative charge. Therefore, these features depend not only on the molecular architecture of the network but also on the conditions of the environment.

Far from the film (large z), the degree of charge of histidine is that of the bulk. The last distinctive region is the interface between the film and the bulk solution, where $f_{his}(z)$ goes from $\langle f_{his}\rangle$ to f_{his}^{b} as the distance from the surface increases. These general features are common to all solution compositions. However, in Figure 8 we have chosen a relatively low salt concentration, c = 1 mM, to highlight the fact that the presence of the pH-sensitive adsorbate reduces the thickness of the interfacial region. To illustrate this phenomenon, let us define the local pH as

$$\mathrm{pH}(z) = -\log[\mathrm{H}^{+}(z)] \tag{7}$$

where $[\mathrm{H}^{+}(z)]$ is the local molar concentration of protons. In panel B of Figure 8, we show the local pH as a function of the distance from the surface in both situations, for a solution with 1 mM of his$_6$ and for one without an adsorbate component. As z increases, stars and circles mark the point at which the values of the local and bath pH are within 1% of each other, for the cases with and without his$_6$ in the solution, respectively. We have arbitrarily chosen this value to quantify the position where the interface ends.

The width of the interfacial region correlates with the ionic strength of the bulk solution

$$I_s = \frac{1}{2} \sum_{i \in \text{bulk ionic species}} c_i z_i^{\,2} \tag{8}$$

where the sum runs over all the ionic species in the bulk solution, including protonated histidine residues. The symbol c_i represents the molar concentration of ionic species i and z_i its charge number. The bottom-right inset of Figure 8B shows I_s as a function of the pH. The rest of the conditions are the same as in the main plot and panel A. For the salt solutions of Figure 8B, the interfacial region ends around the same distance from the surface independently of the pH. This behavior occurs because the bulk ionic strength of these solutions is approximately constant within this range of pH (see inset). The lower the ionic strength of the solution, the longer the effective reach of the electrostatic interactions and the

dx.doi.org/10.1021/la5040382 | Langmuir 2014, 30, 15335−15344

extension of the interface. The bulk ionic strength of hexahistidine solutions decreases with increasing pH (in between 6 and 8, see inset), which leads to a longer interface. Stars are tens to almost a hundred nanometers closer to the surface than circles. The interfacial region can be remarkably longer in the absence of the adsorbate species because the bulk ionic strength is lower for salt solutions (more than 1 order of magnitude at pH 6). At pH 8, on the contrary, the ionic strengths of both bulk solutions are similar, and the interfaces end roughly at the same distance from the surface.

Finally, the pH inside the film is always higher for the system containing the peptide, as observed in Figure 8B. Thus, the drop in pH between the bulk and the interior of the film is more significant for salt solutions. This observation is consistent with the results presented in Figure 5A,B, which show that for a hexahistidine solution the degree of dissociation of the network is almost the one expected from bulk considerations, contrary to what occurs for salt solutions.

CONCLUSIONS

We have presented a theoretical study of the adsorption of different molecules within a grafted polyacid hydrogel film in contact with a salt solution of controlled composition. The emphasis has been placed in solutions containing hexahistidine because this peptide has several applications, the most frequent of which is its use as a protein tag in immobilized metal-ion chromatography. To approach the problem, we have employed a molecular theory that explicitly accounts for the conformations of the polymer network, the electrostatic and van der Waals interactions, solvent confinement effects, and the chemical free energy that describes the acid−base equilibrium of all the titratable groups of the system. In addition, the method allows for a molecular-level description of all the components, in particular the adsorbate molecule and the polymer network.

The adsorption of his_6 inside the film shows a nonmonotonic behavior as a function of the solution pH. The acidic units of the network are protonated (uncharged) at low pH, while the residues of the hexamer are uncharged at high pH. Both situations result in no electrostatic attractions between the adsorbate species and the adsorbent macromolecule. Consequently, no adsorption or depletion inside the film is predicted under these conditions. At an intermediate pH range, however, significant adsorption can be observed, which is mainly driven by the electrostatic attractions between the positively charged his_6 and the negatively charged network. The amount of adsorption at a given pH, as well as the pH of maximal adsorption, depends on the salt and adsorbate concentrations and the density of the network. For example, our results suggest that increasing the area density of ionizable polymer is an excellent strategy to increase considerably the adsorption of the histidine tag.

The physicochemical response mechanisms that underlay the observed nonmonotonic adsorption of hexahistidine are not trivial. As a result of the adsorption, the degree of dissociation of the polymer network becomes that of the isolated acid group in a dilute (ideal) solution with the same pH as the bath. Therefore, the contribution to the total free energy from the acid−base equilibrium of the network is near its minimum value. Such a response is unexpected based on the predictions for solutions without his_6, where the degree of charge of the network can be significantly lower than that of the ideal solution. On the other hand, the degree of charge of adsorbed his_6 units can be considerably higher than its bulk value. The magnitude of such shift from the bulk behavior depends critically on the solution pH and salt concentration.

The swelling of the hydrogel, triggered by a raise in the pH, is qualitatively different whether the solution contains or not hexahistidine. In both cases, as the polymer network becomes increasingly charged when the solution pH augments, the intranetwork electrostatic repulsions drive the swelling of the hydrogel. When the bath solution contains no adsorbate, the electric charge of the network is much less than that expected from ideal solution considerations. This effect occurs to reduce the electrostatic repulsions between charged network units. Less dissociation in the polymer backbone, however, comes at the expense of increasing the chemical free energy of the network, which is minimized when the degree of charge is exactly that of the ideal solution. During swelling, the gel incorporates salt ions from the solution, which has two opposing consequences on determining the optimal thickness of the film. Salt ions screen the intranetwork electrostatic repulsions, thus disfavoring swelling. The opposite effect is that such screening allows for more dissociation on the polymer to relax the chemical free energy of the network. This dual role of the salt concentration in modulating the competition between the intranetwork electrostatic repulsions and the network chemical free energy can lead to some interesting behavior, such as the nonmonotonic swelling of the grafted polyacid hydrogel film that we have recently reported.[48] On the contrary, when the solution contains hexahistidine, the degree of dissociation of the network is close to that of the ideal solution. The chemical free energy of the network is almost optimal, implying that there is no competition with the intranetwork electrostatic repulsions. The equilibrium of peptide units, however, undergoes a significant deviation from ideality, thus paying the corresponding chemical free energy price. As a result, the thickness of the hydrogel is roughly a monotonic function of the solution pH. This is one example of the nontrivial interplay between the different contributions to the free energy that determine adsorption. The coupling between molecular organization, physical interactions, and chemical state depends exquisitely on the conditions. Pure hydrogel show a highly nonideal chemical behavior. The presence of adsorbed oligohistidine changes the chemical behavior of the network to be seemingly ideal; however, the adsorbed peptide shows a highly nonideal chemical behavior.

The immobilization and purification of histidine-tagged proteins using IMAC are based on the relatively high affinity and reversibility of the binding interactions between histidine residues and metal ions. We are currently working on incorporating metal−histidine binding in our theoretical approach to study the adsorption behavior for a pH-responsive network functionalized with metal ions. In parallel, our current research efforts concentrate on considering the adsorption of full proteins within the hydrogel. The results presented in this work suggest that the pH sensitivity of the hydrogel can be useful to drive histidine-tagged proteins more efficiently to the interior of the chromatography matrix. We have shown that the equilibrium adsorption of pH-sensitive molecules within the polymer film displays nontrivial features. Consequently, the microscopic information that this work provides can be useful in designing novel, full three-dimensional assays for the immobilization and purification/separation of histidine-tagged proteins.

dx.doi.org/10.1021/la5040382 | Langmuir 2014, 30, 15335−15344

METHODS

To describe the equilibrium adsorption of different species within the polyacid hydrogel film, we have used a theoretical approach that accounts for specific molecular details of both components the polymer network and the adsorbate molecule of interest. This theory explicitly describes the regulation of electric charge by each of the weak electrolyte units of the system. The molecular conformations of the polymer network are incorporated into the theoretical framework using molecular dynamics simulations. The present formalism combines the molecular theory that we have recently used to study the swelling behavior of pH-responsive hydrogel nanofilms,[48,51] with a molecular theory that was developed to investigate protein adsorption on surfaces with grafted polymers.[52] The initial procedure of this methodology consists in writing the total free energy of the system, which is given by

$$F = -TS_{conf} - TS_{mix} + U_{vdw} + U_{st} + F_{chm} + U_{elec} \quad (9)$$

where T is the system temperature and S_{conf} includes the conformational entropy of the adsorbate and that of the flexible polymer network that makes the backbone of the hydrogel. S_{mix} is the translational entropy of the different free species in the solution including the adsorbate molecule, U_{vdw} is total attractive van der Waals interaction, U_{st} is the total repulsive steric (excluded volume) interaction, and U_{elec} is the total electrostatic energy. In addition, the chemical free energy, F_{chm}, accounts for the acid−base equilibrium of all the titratable units of both the polymer network and the adsorbate molecule if the species bears acid or basic groups. Each of these terms of the free energy can be explicitly expressed as a functional of the probability of the different molecular conformations of the network, the local density profiles of the mobile species, the local degree of dissociation/association of every ionizable species, and the position-dependent electrostatic potential. Optimization of the total free energy with respect to the aforementioned functions leads to a series of equations that can be solved numerically to obtain the local interaction fields (the osmotic pressure and the electrostatic potential). All structural properties can be determined from the probabilities and interaction fields obtained from the optimized free energy. Any thermodynamic quantity of interest can be computed by taking the adequate derivative of the proper thermodynamic potential. Technical details and all the relevant equations of the molecular theory can be found in the Supporting Information and in our previous works.[47,48]

ASSOCIATED CONTENT

Supporting Information

Thorough description of the molecular theory of pH-responsive hydrogels and its extension to study the equilibrium adsorption of ionic and ionizable species; details of the molecular models used to describe the grafted polyacid network and the different adsorbate species considered in this work; additional results. This material is available free of charge via the Internet at http://pubs.acs.org.

AUTHOR INFORMATION

Corresponding Author

*E-mail: igalsz@northwestern.edu (I.S.).

Notes

The authors declare no competing financial interest.

ACKNOWLEDGMENTS

M.O. thanks the support of the Center for Bio-Inspired Energy Science (CBES), which is an Energy Frontier Research Center funded by the U.S. Department of Energy, Office of Science, Office of Basic Energy Sciences, under Award DE-SC0000989. Collaboration for AIDS Vaccine Discovery grant to I.S. (PI: T. Hope) from the Bill and Melinda Gates Foundation (OPP1031734) is acknowledged. I.S. also acknowledges support from NSF (CBET-1264696).

REFERENCES

(1) Tanaka, T.; Fillmore, D.; Sun, S.-T.; Nishio, I.; Swislow, G.; Shah, A. Phase Transitions in Ionic Gels. *Phys. Rev. Lett.* **1980**, *45*, 1636−1639.

(2) Zhao, B.; Moore, J. S. Fast pH- and Ionic Strength-Responsive Hydrogels in Microchannels. *Langmuir* **2001**, *17*, 4758−4763.

(3) De, S.; Aluru, N.; Johnson, B.; Crone, W.; Beebe, D.; Moore, J. Equilibrium Swelling and Kinetics of pH-Responsive Hydrogels: Models, Experiments, and Simulations. *J. Microelectromech. Syst.* **2002**, *11*, 544−555.

(4) Peppas, N. A.; Hilt, J. Z.; Khademhosseini, A.; Langer, R. Hydrogels in Biology and Medicine: From Molecular Principles to Bionanotechnology. *Adv. Mater.* **2006**, *18*, 1345−1360.

(5) Kopeček, J. Hydrogel Biomaterials: A Smart Future? *Biomaterials* **2007**, *28*, 5185−5192.

(6) Lee, K. Y.; Mooney, D. J. Hydrogels for Tissue Engineering. *Chem. Rev.* **2001**, *101*, 1869−1880.

(7) Suri, J. T.; Cordes, D. B.; Cappuccio, F. E.; Wessling, R. A.; Singaram, B. Continuous Glucose Sensing with a Fluorescent Thin-Film Hydrogel. *Angew. Chem., Int. Ed.* **2003**, *42*, 5857−5859.

(8) Ehrick, J. D.; Luckett, M. R.; Khatwani, S.; Wei, Y.; Deo, S. K.; Bachas, L. G.; Daunert, S. Glucose Responsive Hydrogel Networks Based on Protein Recognition. *Macromol. Biosci.* **2009**, *9*, 864−868.

(9) Zhang, X.; Guan, Y.; Zhang, Y. Ultrathin Hydrogel Films for Rapid Optical Biosensing. *Biomacromolecules* **2011**, *13*, 92−97.

(10) Mateescu, A.; Wang, Y.; Dostalek, J.; Jonas, U. Thin Hydrogel Films for Optical Biosensor Applications. *Membranes* **2012**, *2*, 40−69.

(11) Wu, W.; Mitra, N.; Yan, E. C. Y.; Zhou, S. Multifunctional Hybrid Nanogel for Integration of Optical Glucose Sensing and Self-Regulated Insulin Release at Physiological pH. *ACS Nano* **2010**, *4*, 4831−4839.

(12) Qiu, Y.; Park, K. Environment-Sensitive Hydrogels for Drug Delivery. *Adv. Drug Delivery Rev.* **2001**, *53*, 321−339.

(13) Oh, J. K.; Drumright, R.; Siegwart, D. J.; Matyjaszewski, K. The Development of Microgels/Nanogels for Drug Delivery Applications. *Prog. Polym. Sci.* **2008**, *33*, 448−477.

(14) Hamidi, M.; Azadi, A.; Rafiei, P. Hydrogel Nanoparticles in Drug Delivery. *Adv. Drug Delivery Rev.* **2008**, *60*, 1638−1649.

(15) Kabanov, A. V.; Vinogradov, S. V. Nanogels as Pharmaceutical Carriers: Finite Networks of Infinite Capabilities. *Angew. Chem., Int. Ed.* **2009**, *48*, 5418−5429.

(16) Raemdonck, K.; Demeester, J.; De Smedt, S. Advanced Nanogel Engineering for Drug Delivery. *Soft Matter* **2009**, *5*, 707−715.

(17) Sasaki, Y.; Akiyoshi, K. Nanogel Engineering for New Nanobiomaterials: From Chaperoning Engineering to Biomedical Applications. *Chem. Rec.* **2010**, *10*, 366−376.

(18) Sasaki, Y.; Kazunari, A. In *Hydrogel Micro and Nanoparticles*; Lyon, A. L., Serpe, M. J., Eds.; Wiley-VCH: Weinheim, Germany, 2012; Chapter 8.

(19) Lowman, A. M.; Morishita, M.; Kajita, M.; Nagai, T.; Peppas, N. A. Oral Delivery of Insulin Using pH-Responsive Complexation Gels. *J. Pharm. Sci.* **1999**, *88*, 933−937.

(20) Morishita, M.; Lowman, A. M.; Takayama, K.; Nagai, T.; Peppas, N. A. Elucidation of the Mechanism of Incorporation of Insulin in Controlled Release Systems Based on Complexation Polymers. *J. Controlled Release* **2002**, *81*, 25−32.

(21) Torres-Lugo, M.; Peppas, N. A. Molecular Design and In Vitro Studies of Novel pH-Sensitive Hydrogels for the Oral Delivery of Calcitonin. *Macromolecules* **1999**, *32*, 6646−6651.

(22) Torres-Lugo, M.; García, M.; Record, R.; Peppas, N. A. Physicochemical Behavior and Cytotoxic Effects of p(Methacrylic Acid-g-Ethylene Glycol) Nanospheres for Oral Delivery of Proteins. *J. Controlled Release* **2002**, *80*, 197−205.

(23) Biswas, E. E.; Chen, P.-h.; Biswas, S. B. Overexpression and Rapid Purification of Biologically Active Yeast Proliferating Cell Nuclear Antigen. *Protein Expression Purif.* **1995**, *6*, 763−770.

(24) Porath, J.; Carlsson, J.; Olsson, I.; Belfrage, G. Metal Chelate Affinity Chromatography, a New Approach to Protein Fractionation. *Nature* **1975**, *258*, 598−599.
(25) Gentz, R.; Chen, C. H.; Rosen, C. A. Bioassay for Trans-Activation Using Purified Human Immunodeficiency Virus Tat-Encoded Protein: Trans-Activation Requires mRNA Synthesis. *Proc. Natl. Acad. Sci. U. S. A.* **1989**, *86*, 821−824.
(26) Paborsky, L. R.; Dunn, K. E.; Gibbs, C. S.; Dougherty, J. P. A Nickel Chelate Microtiter Plate Assay for Six Histidine-Containing Proteins. *Anal. Biochem.* **1996**, *234*, 60−65.
(27) Sigal, G. B.; Bamdad, C.; Barberis, A.; Strominger, J.; Whitesides, G. M. A Self-Assembled Monolayer for the Binding and Study of Histidine-Tagged Proteins by Surface Plasmon Resonance. *Anal. Chem.* **1996**, *68*, 490−497.
(28) Schmid, E. L.; Keller, T. A.; Dienes, Z.; Vogel, H. Reversible Oriented Surface Immobilization of Functional Proteins on Oxide Surfaces. *Anal. Chem.* **1997**, *69*, 1979−1985.
(29) Rigler, P.; Ulrich, W.-P.; Hoffmann, P.; Mayer, M.; Vogel, H. Reversible Immobilization of Peptides: Surface Modification and In Situ Detection by Attenuated Total Reflection FTIR Spectroscopy. *ChemPhysChem* **2003**, *4*, 268−275.
(30) Miyazaki, M.; Kaneno, J.; Yamaori, S.; Honda, T.; Briones, M. P. P.; Uehara, M.; Arima, K.; Kanno, K.; Yamashita, K.; Yamaguchi, Y.; Nakamura, H.; Yonezawa, H.; Fujii, M.; Maeda, H. Efficient Immobilization of Enzymes on Microchannel Surface Through His-Tag and Application for Microreactor. *Protein Pept. Lett.* **2005**, *12*, 207−210.
(31) Tachibana, S.; Suzuki, M.; Asano, Y. Application of an Enzyme Chip to the Microquantification of l-Phenylalanine. *Anal. Biochem.* **2006**, *359*, 72−78.
(32) Kang, E.; Park, J.-W.; McClellan, S. J.; Kim, J.-M.; Holland, D. P.; Lee, G. U.; Franses, E. I.; Park, K.; Thompson, D. H. Specific Adsorption of Histidine-Tagged Proteins on Silica Surfaces Modified with Ni^{2+}/NTA-Derivatized Poly(Ethylene Glycol). *Langmuir* **2007**, *23*, 6281−6288.
(33) Cassimjee, K. E.; Trummer, M.; Branneby, C.; Berglund, P. Silica-Immobilized His6-Tagged Enzyme: Alanine Racemase in Hydrophobic Solvent. *Biotechnol. Bioeng.* **2008**, *99*, 712−716.
(34) Shi, X.-W.; Wu, H.-C.; Liu, Y.; Tsao, C.-Y.; Wang, K.; Kobatake, E.; Bentley, W. E.; Payne, G. F. Chitosan Fibers: Versatile Platform for Nickel-Mediated Protein Assembly. *Biomacromolecules* **2008**, *9*, 1417−1423.
(35) Yu, T.; Wang, Q.; Johnson, D. S.; Wang, M. D.; Ober, C. K. Functional Hydrogel Surfaces: Binding Kinesin-Based Molecular Motor Proteins to Selected Patterned Sites. *Adv. Funct. Mater.* **2005**, *15*, 1303−1309.
(36) Kibrom, A.; Roskamp, R. F.; Jonas, U.; Menges, B.; Knoll, W.; Paulsen, H.; Naumann, R. L. C. Hydrogel-Supported Protein-Tethered Bilayer Lipid Membranes: A New Approach Toward Polymer-Supported Lipid Membranes. *Soft Matter* **2011**, *7*, 237−246.
(37) Arvidsson, P.; Plieva, F. M.; Lozinsky, V. I.; Galaev, I. Y.; Mattiasson, B. Direct Chromatographic Capture of Enzyme from Crude Homogenate Using Immobilized Metal Affinity Chromatography on a Continuous Supermacroporous Adsorbent. *J. Chromatogr. A* **2003**, *986*, 275−290.
(38) Efremenko, E.; Votchitseva, Y.; Plieva, F.; Galaev, I.; Mattiasson, B. Purification of His6-Organophosphate Hydrolase Using Monolithic Supermacroporous Polyacrylamide Cryogels Developed for Immobilized Metal Affinity Chromatography. *Appl. Microbiol. Biotechnol.* **2006**, *70*, 558−563.
(39) Asayama, W.; Sawada, S.-i.; Taguchi, H.; Akiyoshi, K. Comparison of Refolding Activities Between Nanogel Artificial Chaperone and GroEL Systems. *Int. J. Biol. Macromol.* **2008**, *42*, 241−246.
(40) Sawada, S.-i.; Akiyoshi, K. Nano-Encapsulation of Lipase by Self-Assembled Nanogels: Induction of High Enzyme Activity and Thermal Stabilization. *Macromol. Biosci.* **2010**, *10*, 353−358.
(41) Ha, E.-J.; Kim, Y.-J.; An, S. S. A.; Kim, Y.-R.; Lee, J.-O.; Lee, S.-G.; Paik, H.-j. Purification of His-Tagged Proteins Using Ni2+−Poly(2-Acetamidoacrylic Acid) Hydrogel. *J. Chromatogr. B* **2008**, *876*, 8−12.
(42) Ha, E.-J.; Kim, B.-S.; Park, E.-K.; Song, K.-W.; Lee, S.-G.; An, S. S. A.; Paik, H.-j. Site-Specific Reversible Immobilization and Purification of His-Tagged Protein on Poly(2-Acetamidoacrylic Acid) Hydrogel Beads. *Polym. Adv. Technol.* **2013**, *24*, 75−80.
(43) Ha, E.-J.; Kim, K. K.; Park, H. S.; Lee, S.-G.; Lee, J.-O.; An, S. S. A.; Paik, H.-j. One-Step Immobilization and Purification of His-Tagged Enzyme Using Poly(2-Acetamidoacrylic Acid) Hydrogel. *Macromol. Res.* **2013**, *21*, 5−9.
(44) Lin, C.-C.; Metters, A. T. Metal-Chelating Affinity Hydrogels for Sustained Protein Release. *J. Biomed. Mater. Res., Part A* **2007**, *83A*, 954−964.
(45) Lin, C.-C.; Metters, A. T. Bifunctional Monolithic Affinity Hydrogels for Dual-Protein Delivery. *Biomacromolecules* **2008**, *9*, 789−795.
(46) Puri, M.; Kaur, A.; Singh, R. S.; Schwarz, W. H.; Kaur, A. One-Step Purification and Immobilization of His-Tagged Rhamnosidase for Naringin Hydrolysis. *Process Biochem.* **2010**, *45*, 451−456.
(47) Longo, G. S.; Olvera de la Cruz, M.; Szleifer, I. Molecular Theory of Weak Polyelectrolyte Gels: The Role of pH and Salt Concentration. *Macromolecules* **2011**, *44*, 147−158.
(48) Longo, G. S.; Olvera de la Cruz, M.; Szleifer, I. Non-Monotonic Swelling of Surface Grafted Hydrogels Induced by pH and/or Salt Concentration. *J. Chem. Phys.* **2014**, *141*, 124909.
(49) Lide, D. R., Ed.; *CRC Handbook of Chemistry and Physics*, 90th ed.; CRC Press/Taylor and Francis: Boca Raton, FL, 2010.
(50) Flory, P. J. *Statistical Mechanics of Chain Molecules*; Wiley-Interscience: New York, 1969.
(51) Longo, G. S.; Olvera de la Cruz, M.; Szleifer, I. Molecular Theory of Weak Polyelectrolyte Thin Films. *Soft Matter* **2012**, *8*, 1344−1354.
(52) Szleifer, I. Protein Adsorption on Surfaces with Grafted Polymers. *Biophys. J.* **1997**, *72*, 595−612.